RHESSI OBSERVATION OF FLARE ELEMENTS

Paolo C. Grigis and Arnold O. Benz

Institute for Astronomy, ETH Zürich, 8092 Zürich, Switzerland

ABSTRACT

RHESSI observations of *elementary flare bursts* are presented. These solar flare elements are distinct emission peaks of a duration of some tens of seconds present in the hard X-ray light curves. They are characterized by consistent soft-hard-soft spectral behavior, which can be described in a quantitative way and compared which predictions from acceleration models. A detailed analysis of hard X-ray images for an M5 class flare shows that elementary flare bursts do not occur at distinct locations, but as twin X-ray sources move smoothly along an arcade of magnetic loops. This observation apparently contradicts the predictions of standard translation invariant 2.5-dimensional reconnection models.

1. INTRODUCTION

The hard X-ray emission from solar flares at energies higher than about 25 keV is strongly variable in intensity and often it is possible to recognize several distinct emission peaks, lasting from a few seconds to several minutes. Following de Jager & de Jonge (1978), we will call these peaks in the light curve Elementary Flare Bursts (EFB) or, shortly, flare elements. In the usual interpretation, non-thermal electrons accelerated in the corona are responsible for the X-ray emission as they precipitate into the lower, denser layers of the solar atmosphere and emit bremsstrahlung at the footpoints (FP) of magnetic loops. Therefore, the variation in the intensity of the X-ray light curves seen during an EFB reflects a change in the flux of accelerated electrons, which can be accounted for by a variation in the power of the accelerator, or a change in the efficiency of the release of particles trapped in the corona.

The *RHESSI* satellite (Lin et al., 2002) provides light curves, spectra and images. The interplay between these different sources of information allows us to characterize the EFB in a much more detailed way than purely temporal studies from light curves. The temporal evolution of the spectra shows that the hardness of the photon spectrum changes during a flare element, reaching
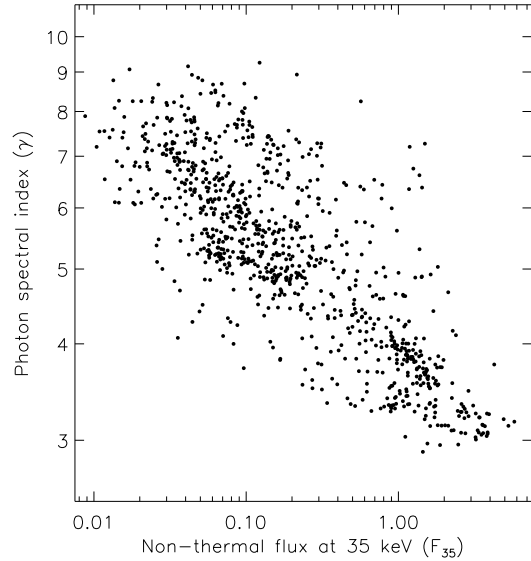

Figure 1. Spectral index (γ) versus the fitted non-thermal flux at 35 keV (F_{35}, given in photons s^{-1} cm^{-2} keV^{-1}), for all 4 s intervals during 24 flares.

its maximum at peak time. This behavior is called Soft-Hard-Soft (SHS), and has been known for decades (Parks and Winckler, 1969). It has recently been studied in a more quantitative way by Grigis & Benz (2004) and Grigis & Benz (2005).

Images of flare sources above 25 keV usually show one or more sources, typically coming from footpoints of magnetic loops. Two FPs on opposite sides of a magnetic neutral line are expected in the standard model of eruptive flares (reviewed, e.g., by Priest & Forbes 2002). The rapid eruption of a cusp-shaped filament enables the magnetic field to reconnect, driving particle acceleration in field lines moving into the cusp. Electrons precipitate to the FPs of these field lines in the chromosphere. In this scenario, one expects the observed FP sources to drift apart as successive field lines are reconnected at higher altitudes. This explanation fits the long-known outward motion of Hα ribbons parallel to the neutral line. How-
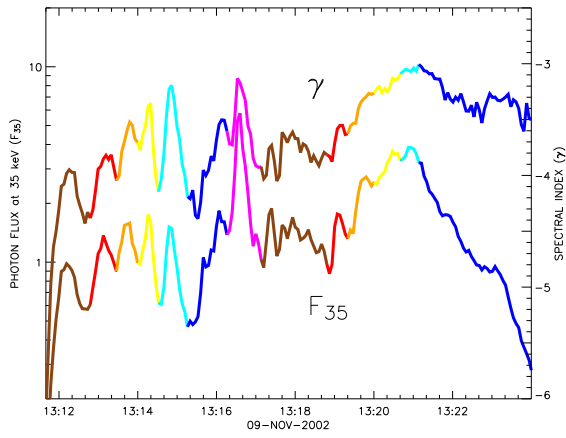
Figure 2. Time evolution of the non-thermal photon flux at 35 keV (F_{35}) and the spectral index (γ).

ever, observations reveal a more complex picture, where source motion can be as well parallel to the neutral line (Bogachev, 2005). If the standard model of the solar flares holds for an EFB, it predicts systematic outward motions of the FP sources during a flare element, while erratic jumps are expected between EFBs, as different loop system are triggered into a phase of strong particle acceleration and energy release.

Here we report observations of the general behavior of flare elements, discussing them in more detail for one event showing continuous motion along the ribbon of the arcade. The question of the specific motion during flare elements is addressed in detail.

2. SPECTRAL EVOLUTION OF THE FLARE ELEMENTS

The spectral evolution for the EFBs is studied by producing high cadence (4 s) spectral fittings to the incoming photons. The fitted model consist of two components: an emission from an isothermal plasma and a non-thermal power-law spectrum. The first dominates at low energies (< 25 keV). We are interested on the temporal development of the second component, which is parameterized by its spectral index γ and its normalization F_{35} (that is, the strength of the photon flux at 35 keV, given in photons s^{-1} cm^{-2} keV^{-1}). Assuming a thick target model for the bremsstrahlung-producing collisions of non-thermal electron with the cold ambient plasma, the electron flux is still a power law with spectral index $\delta = \gamma + 1$ and its normalization can be easily computed.

The results of a set of fittings as the ones described above from a sample of 24 uniformly selected flares in the time period February-November 2002, ranging in size from GOES class M1 to X1, are shown in Fig. 1. There is an evident trend correlating stronger flux with lower spectral index. This shows an overall SHS effect. The ef-
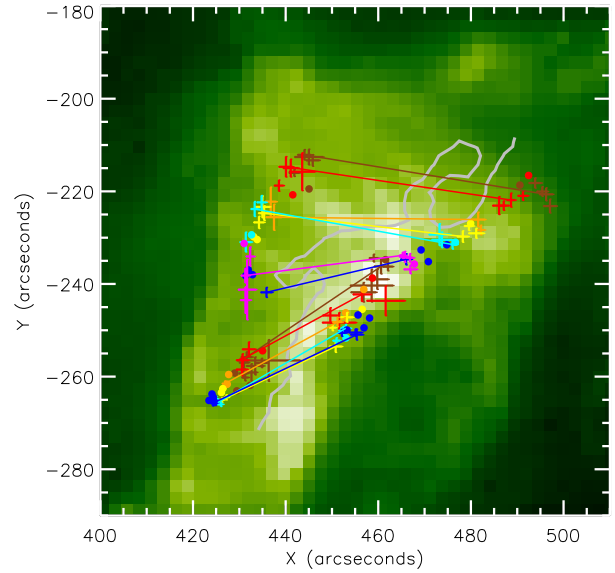

Figure 3. SOHO EIT 195 Å image of postflare loops with the RHESSI HXR source positions superimposed. The positions of the 20–50 keV sources from the CLEAN images are represented by crosses with arm lengths proportional to the errors, positions from the PIXON images are given by circles. Simultaneous FPs are connected and color coded according to the time intervals defined in Fig. 2

fect however, holds not only as a general trend between small and large flares (Battaglia, Grigis, & Benz, 2005), but also during single flare elements. This is exemplified by the flare of November 9, 2002. Figure 2 shows the evolution of the normalization of the non-thermal component at 35 keV (lower curve) and the spectral index (upper curve). The colors have been chosen to highlight the different flare elements. It is evident that the SHS effect is more pronounced in each EFB than in the flare as a whole.

To be able to follow the evolution of the single EFBs in more details, aiming for a more quantitative description of the effect, we switch to the electron spectra. The quantitative analysis of 70 rise and decay phases of flare elements belonging to the 24 selected flares show that the electron spectra in a rise or decay phase can be approximately described by having a common point of intersection, a *pivot point*. The exact location of the pivot point in the flux vs. energy diagram may be different for each element, and also from the rise phase to the decay phase, but the distribution of the pivot point energy ϵ_{PIV} for all the rise and decay phases lies mainly between 10 keV and 30 keV and is centered around 20 keV. An asymmetry between the rise and decay phases is seen: the spectra tend to harden with a faster rate in the rise phase than they soften with decreasing flux.

The presence of a pivot point leads to an SHS effect at energies larger than the pivot point energy and to an hard-soft-hard behavior at lower energies. We note that the
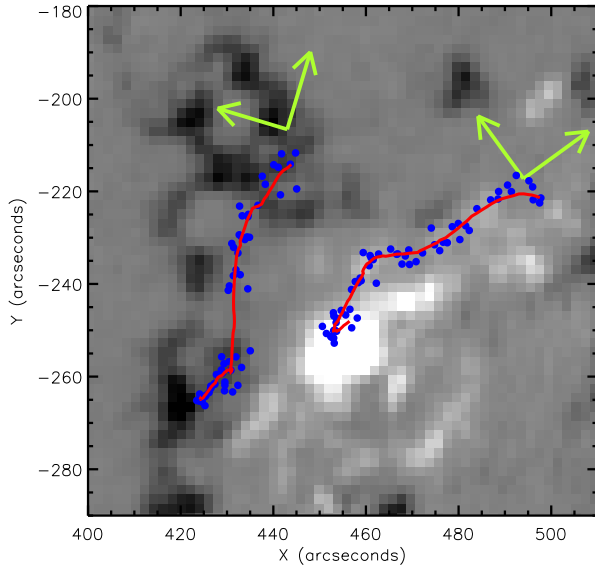
Figure 4. SOHO *MDI magnetogram with the RHESSI PIXON source position superimposed (blue circles). The red lines represent the smoothed trend line for the source motions. The green arrows denote the* parallel *and* perpendicular *directions with respect to the two ribbons.*

converse is not true: it is possible to build a set of spectra showing the SHS effect at, say, 35 keV which do not have a common point of intersection (for example, if all the spectra were tangent to the same parabola).

A pivot point and SHS behavior can, at least approximately, be realized by holding constant the number of electrons accelerated per second over a threshold energy, or by the stochastic acceleration scenario proposed by Benz (1977) and Brown & Loran (1985). The authors are working on a comparison of the spectral behavior with the prediction from more sophisticated stochastic acceleration models.

3. LOCATION OF THE FLARE ELEMENTS

The non-thermal electrons responsible for the power-law component of the photon spectra are seen in hard X-ray images as loop footpoints. We study in more detail the motion of the FP sources in the event of November 9, 2002. This is an M5 class flare showing a pronounced post-flare loop arcade in EIT images at 195 Å. We produced a series of RHESSI images with 8 second cadence, using the CLEAN and the PIXON reconstruction algorithms.

The morphology of the hard X-ray images show two sources located at opposite sites of the magnetic neutral line for most images. In some images only one source is clearly defined. The source position was computed from a fitting of a two-dimensional elliptical Gaussian to each
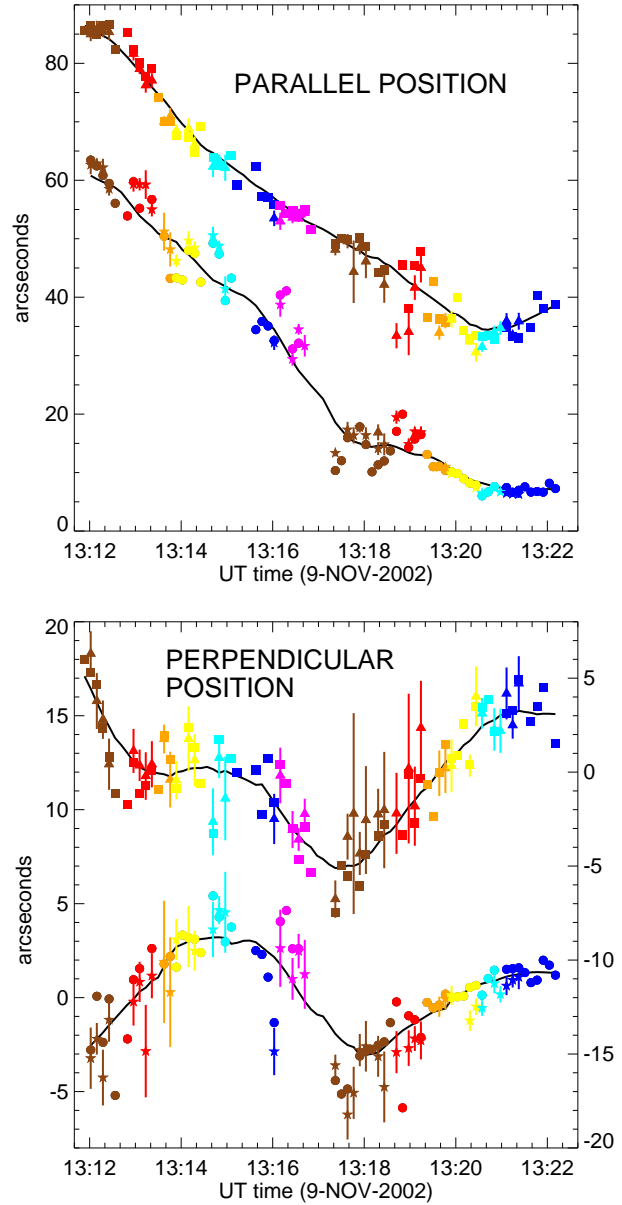

Figure 5. Time evolution of the source positions relative to the trend lines. The color code is the same as in Fig. 1, referring to the major subpeaks. Triangles and stars with error bars refer to values derived using CLEAN, squares and circles using PIXON, for the western and eastern FPs, respectively. Top: The upper curve displays the parallel coordinates of the western FPs; the lower curve shows the same, but for the eastern FPs. Bottom: Time evolution of the coordinate perpendicular to the regression lines. The upper curve refers to the western FP (scale on the right), the lower curve to the eastern FP (scale on the left). Both panels show in black the averaged smoothed motion for each FP (PIXON value), defining a new reference for detailed analysis presented in Fig. 6
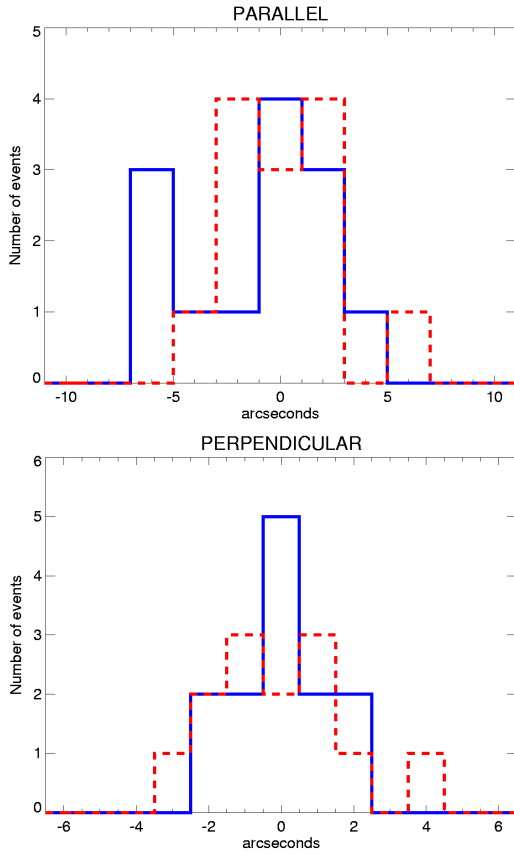
PARALLEL

PERPENDICULAR

Figure 6. Distribution of the average motions during a flare element in perpendicular and parallel directions relative to the time averaged trend curves. Eastern FPs are shown with continuous blue lines, western FP with dashed red lines.

visible source separately.

The source positions are shown on Fig. 3, overlaid on an EIT image at 195 Å showing the loop arcade. They are also reported on Fig. 4 as an overlay on an MDI magnetogram. The red trend lines in Fig. 4 represent the position of the sources smoothed with a moving average using a smoothing window corresponding to a duration of 120 s, much longer than the individual duration of an EFB. We now study the characteristics of flare element motion relative to the smooth trend line. Moreover, we decompose the relative positions in two directions, *parallel* and *perpendicular* to the arcade. These directions are obtained from coarse fittings to the eastern and western source positions by straight lines. They are also displayed in Fig. 4.

Do subpeaks show motions perpendicularly outward from the ribbons, as expected from the standard reconnection model? In Fig. 5 (bottom) this is not obvious, although the two FPs are apparently moving relative to the regression line. Note, however, that the lines are converging; thus, the effective FP separation decreases. The standard reconnection model predicts outward FP motion at a given place in the arcade. In order to look for such

systematic trends within HXR subpeaks, we took the parallel and perpendicular components of the difference vector from the smoothed source position to the observed PIXON positions. For each subpeak, we averaged the positions occurring during the first half and the second half of its duration. Then the difference of the second minus the first half, Δ^{POS}, was calculated for both eastern and western sources.

For EFBs produced by standard reconnection, one would expect outward moving sources, thus $\Delta^{\perp}_{\mathrm{POS}}$ being positive, at least on average. Furthermore, the motion along the ribbons should be stepwise and discontinuous with $\Delta^{\parallel}_{\mathrm{POS}}$ being positive if each EFB were a localized event. Fig. 6 demonstrates that these expectations are not satisfied during subpeaks of this flare. The distribution of the average perpendicular motion during each peak shown in Fig. 6 has a mean $\Delta^{\perp}_{\mathrm{POS}}$ value of $0.0'' \pm 0.4$ for the eastern FP and $0.2'' \pm 0.5$ for the western FP (the error is the standard error of the average). The mean value of the relative parallel motion during the peaks is $-1.0'' \pm 1.0$ for the eastern FP and $0.4'' \pm 0.7$ for the western FP.

The global motion along the arcade progresses with an average velocity in the parallel direction of 63 km s^{-1} for the eastern FP and 55 km s^{-1} for the western FP. The lower velocity of the western FP is due to the fact that the last data points have negative parallel velocities since they move backward (Fig. 2). Averaging the absolute values of the parallel component of the velocity, we get 65 km s^{-1} for the western FP. A speed of about 110 km s^{-1} is maintained for 2 minutes in the western FP at the beginning of the flare, while the data gap and possible jump around 13:17 in the eastern FP position requires 180 km s^{-1}.

Since the ultimate energy source of a flare is provided by the magnetic field, we expect that is possible to accelerate more particles in regions of the arcade where stronger magnetic fields are present. It is possible to measure photospheric magnetic fields routinely, but we don't have easy access to the values of coronal magnetic fields. Extrapolations are possible, but neglects the effect of coronal currents. Nevertheless, we can check whether there is a correlation in our data between the photospheric magnetic field strength and the hard X-ray flux (Fig. 7).

We take the field values from SOHO/MDI line-of-sight magnetograms using the value of the MDI pixel nearest to the PIXON centroid position of the footpoint sources. For the western FP, there is a general trend of increase in the magnetic field strength after 13:19, where the photon flux also get larger. This is not seen for the eastern FP. This is confirmed by the values of the cross correlation coefficients R_{W} and R_{E} for the western and eastern FP, respectively. We have $R_{\mathrm{W}} = 0.60^{+0.08+0.14}_{-0.09-0.19}$ and $R_{\mathrm{W}} = 0.19^{+0.12+0.23}_{-0.13-0.26}$, where the errors indicate the interval for the 68.3% and 95.5% confidence level, respectively. However, if we compute the correlation coefficients separately for each EFB and the build the average, we get lower values $\overline{R}_{\mathrm{W}} = 0.24 \pm 0.17 \pm 0.36$ and $\overline{R}_{\mathrm{E}} = 0.12 \pm 0.20 \pm 0.43$. In Fig. 7 we see that
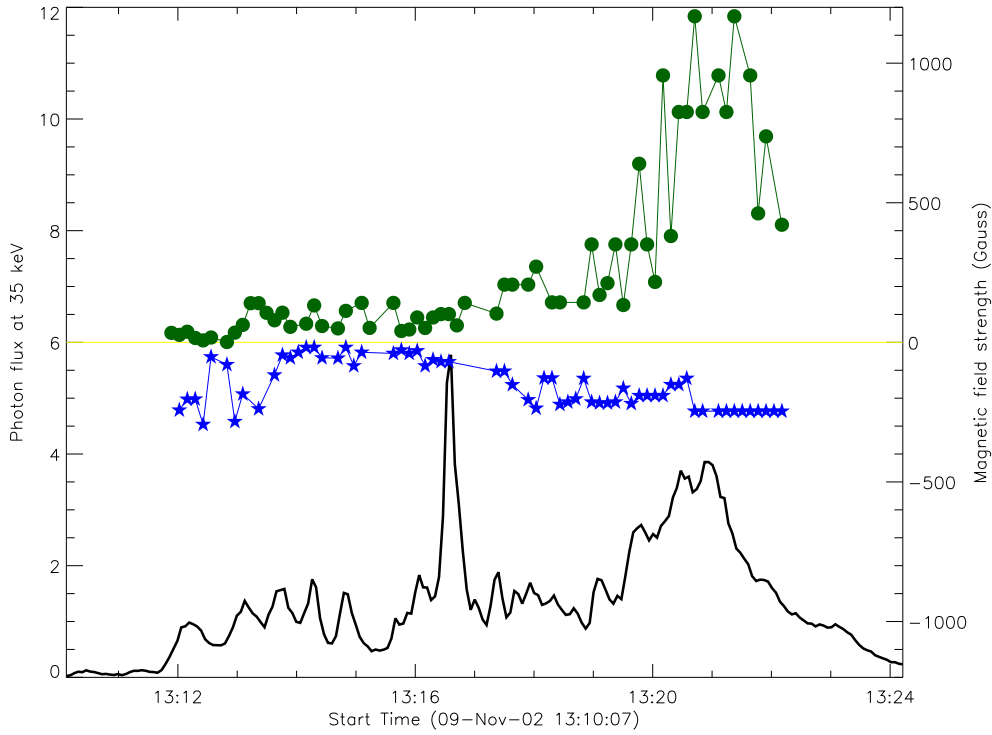
Figure 7. Magnetic field strength encountered by the FP sources (top) and photon flux at 35 keV (bottom) vs. time. The photospheric field measured by SOHO/MDI (Fig. 4) shown with green circles stands for the western FPs, the blue asterisks represent the eastern FPs.

the strongest peak happens in a region of weak magnetic field. The data suggest that the effect of the magnetic field can be seen in the overall, gradual progression of the flare, but not for the impulsive flare elements. This indicates that the plasma responsible for the local acceleration and energy release in the loops may be dominated by region of strong currents and/or turbulence and that the pre-flare conditions of the magnetic field are far from a potential state.

4. CONCLUSION

The flare elements seen very often in impulsive flares can be identified in the lightcurves, but have also well defined spectral behavior. The quantitative analysis of the behavior can be compared with predictions from acceleration models, which must be able to account not only for a general soft-hard-soft behavior, but also for the presence of an approximate pivot point in the electron spectra. The consistent spectral behavior of the flare elements may suggest that they constitute independent units representing separate acceleration events during the flare.

The hard X-ray images for the event of November 9, 2002 confirm this view partially as the different elements are found at spatially distinct locations on the arcade. Different loops are active at different times. Surprisingly, the

footpoints move smoothly along the two ribbons, however, in contrast with the bursty evolution of the hard X-ray flux. The parallel source motions exclude the generally held notion of EFBs being the modulation of a global reconnection process. Instead, the temporal modulation of the HXR flux and spectral index appear to be caused by a spatial displacement along the arcade. This could be caused by some disturbance propagating smoothly along the arcade, sequentially triggering a reconnection process in successive loops of the arcade. The disturbance would have to propagate with a speed in the range 50–150 km s^{-1}, much lower than the Alfvén velocity.

In the impulsive phase of this flare, magnetic energy release appears not in the form of a quasi-steady reconnection annihilating antiparallel magnetic field and thus producing outward moving FPs. The main flare energy release at a given position in the arcade seems to last only a short time (order of a few seconds) and moves along the arcade in a systematic manner. The observed modulation of the HXR flux and the related anticorrelation of the spectral index in each EFB appear to be caused by spatial variations of the acceleration efficiency. The temporal variations thus seem to be the result of a continuously moving trigger propagating through variable conditions in the arcade. The short lifetime of an FP at a given position shows that particle trapping is not effective over timescales larger than several tens of seconds.

The observed simple and systematic motions set this event apart as a prototype for a type of HXR flare evolving along the arcade. The FP motions of this flare clearly contradict the expectations of the standard two-dimensional reconnection model. The fact that we do not observe a systematic increase (up to the instrumental limits) of the separation of the FPs does challenge the idea that the reconnection points move upward, and particles are accelerated in field lines successively farther out during the main HXR emitting phase of the flare. A possible interpretation is that the trigger releases the main energy stored in a two-dimensional loop structure within seconds, without noticeable FP motion, and moves on. Reconnection in the given structure may still continue, but with HXR emission below RHESSI sensitivity and at a much reduced energy release rate.

We thus propose a scenario in which a disturbance, probably connected to the eruption of a filament, propagates along the arcade like a burning fuse, sequentially triggering reconnection and particle acceleration in the flare loops. The main HXR emission from the FP reflects the propagation of this disturbance, not the reconnection process at a given place in the arcade. If the dominating emission is strong and short-lived, the local conditions cause the observed temporal modulation.

The global evolution may be compatible with the standard model of an eruptive flare, if one allows the filament to erupt in such a way that one of its ends does not move while the other starts to rise. In this scenario the reconnection process spreads along the arcade until it reaches the end. The arcade erupts in a manner similar to the opening of a zipper, where the lower side run across the arcade and the upper side is the filament. Future studies of HXR FPs in a large number of flares may establish such a scenario and stimulate the development of three-dimensional reconnection models needed to understand these observations.

ACKNOWLEDGMENTS

REFERENCES

Battaglia, M., Grigis, P. C., & Benz, A. O. Size dependence of solar X-ray flare properties, 2005, A&A, 439, 737

Benz, A. O. Spectral features in solar hard X-ray and radio events and particle acceleration, 1977, ApJ, 211, 270

Bogachev, S. A., Somov, B. V., Kosugi, T., & Sakao, T. The motions of the hard X-ray sources in solar flares: images and statistics, 2005, ApJ, 630, 561

Brown, J. C., & Loran, J. M. Possible evidence for stochastic acceleration of electrons in solar hard X-ray bursts observed by SMM, 1985, MNRAS, 212, 245

de Jager, C., & de Jonge, G. Properties of elementary flare bursts, 1978, Sol. Phys., 58, 127

Grigis, P. C., & Benz, A. O. The spectral evolution of impulsive solar X-ray flares , 2004, A&A, 426, 1093

Grigis, P. C., & Benz, A. O. The spectral evolution of impulsive solar X-ray flares. II. Comparison of observations with models , 2005, A&A, 434, 1173

Grigis, P. C., & Benz, A. O. The Evolution of Reconnection along an Arcade of Magnetic Loops, 2005, ApJ, 625, L143

Lin, R. P., et al. The Reuven Ramaty High-Energy Solar Spectroscopic Imager (*RHESSI*), 2002, Sol. Phys., 210, 3

Parks, G. K., & Winckler, J. R. Sixteen-Second Periodic Pulsations Observed in the Correlated Microwave and Energetic X-Ray Emission from a Solar Flare, 1969, ApJ, 155, L117